SLAC-PUB-2943
June 1982
(M)

Recent Results from MARK II[1] at PEP*

Presented by D. Schlatter
Stanford Linear Accelerator Center
Stanford University, Stanford, California 94305

Results on hadronic final states in e^+e^- annihilation are reported. The data were collected with the MARK II detector at the PEP storage ring at the Stanford Linear Accelerator Center, operating at a center-of-mass energy of $\sqrt{s}$=29 GeV. The MARK II detector, a 4.5 KG solenoid with cylindrical drift chambers, surrounded by a liquid argon calorimeter, has been described in detail in ref. 2. Hadronic events are selected by applying several cuts. There have to be at least 5 charged particles, each with momentum greater than 100 MeV, in an event. The total visible energy has to be larger than 8 GeV (or 15 Gev in the case of the energy correlation). The vertex position has to coincide with the beam crossing point. The data used for this report correspond to a total integrated luminosity of about 15 pb^{-1} collected in spring 1981.

I. The total cross section.

The total hadronic cross section at $\sqrt{s}$ = 29 GeV as expressed in terms of $R=\sigma_{had}/\sigma_{\mu\mu}$ is R=3.90±0.05 (statistical)±0.25 (systematic). Table I gives measurements of R from the MARK II detector at SPEAR[3] and PEP.

Talk given at the 5th International Vanderbilt High Energy Conference, May 24 - 26, 1982, Nashville, TN.

---

*. Work supported in part by the Department of Energy, contracts DE-AC03-76SF00515, W-7405-ENG-48, and DE-AC02-76ER03064.

Table I. $R=\sigma_{had}/\sigma_{\mu\mu}$ with the MARK II detector
The systematic error is 6% in all cases.

$\sqrt{s}$ (GeV)	R	# events
5.2	3.90 ± 0.02	44180
6.5	3.95 ± 0.05	11900
29.0	3.90 ± 0.05	4750

Within the systematic uncertainty of 6% there is no variation of R in the energy range from 5.2 to 29 GeV. The systematic error comes from the uncertainties in the background subtraction, event selection, radiative corrections and the luminosity measurements. The expected variations of R with energy are of the same order of magnitude (10% due to the onset of bottom production, 5% due to gluon bremsstrahlung and 3% due to electro weak interference) as the systematic uncertainty.

II. The inclusive hadron spectrum.

The inclusive cross section for hadrons, $s d\sigma/dx$, ($x = 2P/\sqrt{s}$) has been measured[4] both at PEP and SPEAR with the MARK II detector (figure 1). The relative uncertainty among the three measurements in the normalization is 10%. Strong scaling violations are observed[4]. At large x the cross section decreases with energy while at small x ($x<0.15$) it increases. In figure 2 the quantity $(1/\sigma d)\sigma/dx$ is plotted as a function of s for different bins of x together with data from the TASSO[5] group at PETRA. There is good agreement between the two experiments given the 10% uncertainty in the relative normalization.

Kinematic effects (in particular from the mass of the charm quark) as well as dynamic effects such as gluon radiation can cause scaling violations[6]. In figure 3 ratios of the inclusive cross sections at 29 GeV and 6.5 GeV from MARK II and at 34 GeV (35 GeV) and 14 GeV from TASSO are shown. A pure perturbative QCD calculation with a scaling parameter Λ = 200 MeV gives the same amount of scaling violations as the data (dashed curve). The sum of the fragmentation function of light quarks and the fragmentation function of the charm quark, folded with the momentum distribution of the light quarks from the charm decay, have been fitted to the data at 6.5 GeV. Then the Altarelli-Parisi equations[7] have been solved numericaly to evolve the spectra to higher energies. Another way to understand the scaling violations is by mean of a cascade Monte Carlo model[8] with single gluon bremsstrahlung. Again, the observed amount of scale breaking is in agreement with these expectations (full line in fig.3). The Monte Carlo model allows us to test the sensitivity of the inclusive hadron spectra to gluon bremsstrahlung. To some surprise the kinematic effects due to finite masses and transverse momenta in a pure $q\bar{q}$ fragmentation model lead to almost the same amount of scale breaking (dotted line) as the $q\bar{q}g$ model (at least from 6.5 GeV to 29GeV). This makes a quantitative analysis of the scale breaking dependent on the details of the model.

III. Energy correlations.

Another general method of probing hadronic final states is the energy correlation measurement[9] proposed by Basham et al.[10] and previously studied by the PLUTO[11] group. The following cross section for the two particle correlation is considered:

$$\frac{1}{\sigma}\frac{d\Sigma}{d\cos\chi} = \frac{1}{N}\frac{1}{\Delta\cos\chi}\sum\sum\frac{E\,E'}{s} \qquad (1)$$

where σ denotes the total cross section and χ the angle between two particles of energy E and E′. The first sum is over all combinations and the second over all N events (note that $(1/\sigma)d\sigma/d\cos\chi$ is normalised to 1). The corrected cross section is shown in figure 4 normalised to the MARK II fiducial volume (70% in the polar angle and 86% in the azimuth). Strong correlations inside a jet ($\chi < 40°$) and between opposite jets ($\chi > 140°$) are observed as expected from a two jet configuration. However this distribution is not symetric around 90° . Figure 5 shows the opposide to same-side asymmetry. Within the model of ref. 10 the energy correlation cross section can be decomposed as follows:

$$\frac{1}{\sigma}\frac{d\Sigma}{d\cos\chi} = \alpha_s A_{q\bar{q}g}^{\text{pert.QCD}}(\chi) + A_{q\bar{q}}^{\text{hadr.}}(\chi) \qquad (2)$$

The first term describes an asymmetric contribution from $q\bar{q}g$ events as calculated in perturbative QCD while the second is symmetric and accounts for the hadronization of $q\bar{q}$ events. At high energies the non perturbative fragmentation term should be down by a factor of $1/\sqrt{s}$ and the $q\bar{q}g$ term should dominate. Possible contributions from fragmentation of $q\bar{q}g$ events are neglected so far. An attempt of a two parameter fit of eq. 2 in the angular range $40° < \chi < 140°$ yields a bad χ^2 (50 for 22 degrees of freedom) with α_s =0.14. To improve the fit we added a third term for possible $q\bar{q}g$ fragmentation. This term has to be asymmetric since for small angles ($\chi < 90°$) the fragmentation is the same as for $q\bar{q}$ events but the corresponding correlation at 180° vanishes in the 3-jet case. We have approximated this third term as follows:

$$A^{hadr.}_{q\bar{q}g}(\chi) = \alpha_s A^{hadr.}_{q\bar{q}}(\chi) \qquad \text{for } \chi < 90°$$

$$= \alpha_s (1+\cos\chi)\ \text{const.} \qquad \text{for } \chi > 90° \qquad (3)$$

A three parameter fit with this extra term yields a better fit (χ^2 = 26 for 21 degrees of freedom) and α_s = 0.19. The result is shown in figures 4 and 5. Obviously there is a strong contribution from fragmentation processes to the asymmetry and thus the determination of α_s is dependent on the fragmentation model.

IV. D* production.

We have searched for D* production[12] in our data in the channel $D^* \rightarrow D^0\pi^+$, $\bar{D} \rightarrow K^+K^-$. No positive particle identification has been used. The time of flight measurement was only required to be consistent with a π or K assumption. The mass resolution does not allow an observation of the D meson in the $K\pi$ mass spectrum. However, if one does a kinematical fit by fixing the $K\pi$ system to the D mass for all events in the interval 1.080 GeV < $M_{K\pi}$ < 1.93GeV , a clear D* signal is observed in the mass difference $M_{K\pi\pi} - M_{K\pi}$ (fig.6). There are 15 D* events at z>0.4 (z=fractional D* energy) above a background of 1 event. The observed D* cross section is rather large ($\sigma(D^*)$ = 0.36± 0.16 nb), but the uncertainty is also large. In fig. 7 the corrected D* production spectrum as a function of the fractional energy, z, is shown. Since D* production from bottom decays is less than 20% and is mainly at small z, most of the events in fig. 7 are from a primary charm quark. Obviously the charm quark fragmentation function is different than the steeply falling light quark fragmentation functions. However, due to the small number of events a flat fragmentation function cannot be ruled out, but the data would prefer a distribution peaked more at the center. A simple model[6] using kinematical considerations for heavy quark fragmentation gives a reasonable describtion of the data (fig 7a). An indirect measurement of a charm fragmentation function has been reported by the CDHS group[13] from $\nu N \to \mu^+\mu^-$hadrons events. They observe a similar distribution with an average z of 0.7 (fig 7b).

Conclusions:

The total cross section ratio R has been measured to within 6%, which is still too large to observe deviations from the quark parton model. The inclusive hadron spectrum shows strong scaling violations in the range of 5.2 GeV < $\sqrt{s}$ < 29 GeV. This is in agreement with cascade QCD Monte Carlo models including fragmentation. However, the energy may be still too low to clearly distinguish between perturbative effects of gluon radiation and non perturbative effects from finite masses. Energy correlation at 29 GeV show an asymmetry as expected from QCD models, but a quantitative result for the strong coupling constant depends on details of the fragmentation model. The observation of D^* production allows a first direct measure of the charm fragmentation function. At present small statistics, only steeply falling spectra are ruled out.

References

1. G.S. Abrams, D. Amidei, A. Bäcker, C.A. Blocker, A. Blondel, Adam M. Boyarski, Martin Breidenbach, D.L. Burke, William Chinowsky, M.W. Coles, G. von Dardel, W.E. Dieterle, J.B. Dillon, J. Dorenbosch, J. Dorfan, M.W. Eaton, G. F. Feldman, M.E.B. Franklin, G. Gidal, L. Gladney, G. Goldhaber, L. Golding, G. Hanson, R.J. Hollebeek, W.R. Innes, J. Jaros, A. Johnson, J.A. Kadyk, A.J. Lankford, Rudolf R. Larsen, B. LeClaire, M.E. Levi, N. Lockyer, B. Löhr, V. Lüth, C. Matteuzzi, M.E. Nelson, J.F. Patrick, Martin L. Perl, Burton Richter, A. Roussarie, D.L. Scharre, H. Schellman, D. Schlatter, R. Schwitters, J. Siegrist, J. Strait, G. H. Trilling, R.A. Vidal, I. Videau, Y. Wang, J. Weiss, M. Werlen, C. Zaiser, G. Zhao Stanford Linear Accelerator Center Stanford University, Stanford, California 94305

Lawrence Berkeley Laboratory and Department of Physics University of California, Berkeley, California 94720

Department of Physics Harvard University, Cambridge, Massachusetts 02138

2. R.H. Schindler et al., Phys. Rev. D24, 78 (1981) and references therin.

3. J. Patrick, Ph.D. Thesis, LBL, 1982.

4. J. Patrick et al. SLAC PUB

5. R. Brandelik et.al., DESY 82-13.

6. C. Peterson et.al., SLAC PUB 2912.

7. G. Altarelli and G. Parisi, Nucl.Phys. B126 (1977)298 and J.

F.Owens,Phys.Lett. 76B,(1978) 85 and T. Uematsu,Phys.Lett. 79B (1978) 97 and E.G. Floratos,C. Kounnas and R. Lacaze,Nucl.Phys. B192 (1981) 417

8. We used the LUND Monte Carlo, T.Sjoestrand LU TP 80-3.

9. D. Schlatter et al.,SLAC PUB 2846.

10. C. Basham, L.Brown, S.Ellis and S. Love, Phys. Rev. D19, 2018 (1979) and Phys. Rev. D24, 2383 (1981).

11. Ch. Berger et al., Phys. Lett. 99B, 292 (1981)

12. J. Yelton et al., SLAC PUB 2926.

13. J. Knobloch, Proc. of International Conference on Neutrino Physics, Maui, Hawaii, 1981.

Figure captions

1. $s d\sigma/dx$ at $\sqrt{s}$ = 5.2 GeV, 6.5Gev and 29GeV.

2. $1/\sigma d\sigma/dx$ from MARK II and TASSO.

3. Ratios of $1/\sigma d\sigma/dx$. a) MARK II for 29 GeV over 6.5Gev. b) TASSO[5] 34 GeV (35GeV) over 14GeV. The full line is from a $q\bar{q}g$ Monte Carlo model, the dotted line is for $q\bar{q}$ two-jet Monte Carlo, the dashed line is an analytic calculation of perturbative QCD.

4. Energy corelation cross section within the MARK II solid angle.

5. Asymetry of the energy correlation.

6. Mass difference $M_{D\pi} - M_D$.

7. Number of D^* events as a function of z.

8. a) D^* spectrum with prediction of ref. 6 (ϵ =0.2). b) Charm fragmentation function from CDHS[13] with prediction of ref. 6 (ϵ = 0.1)

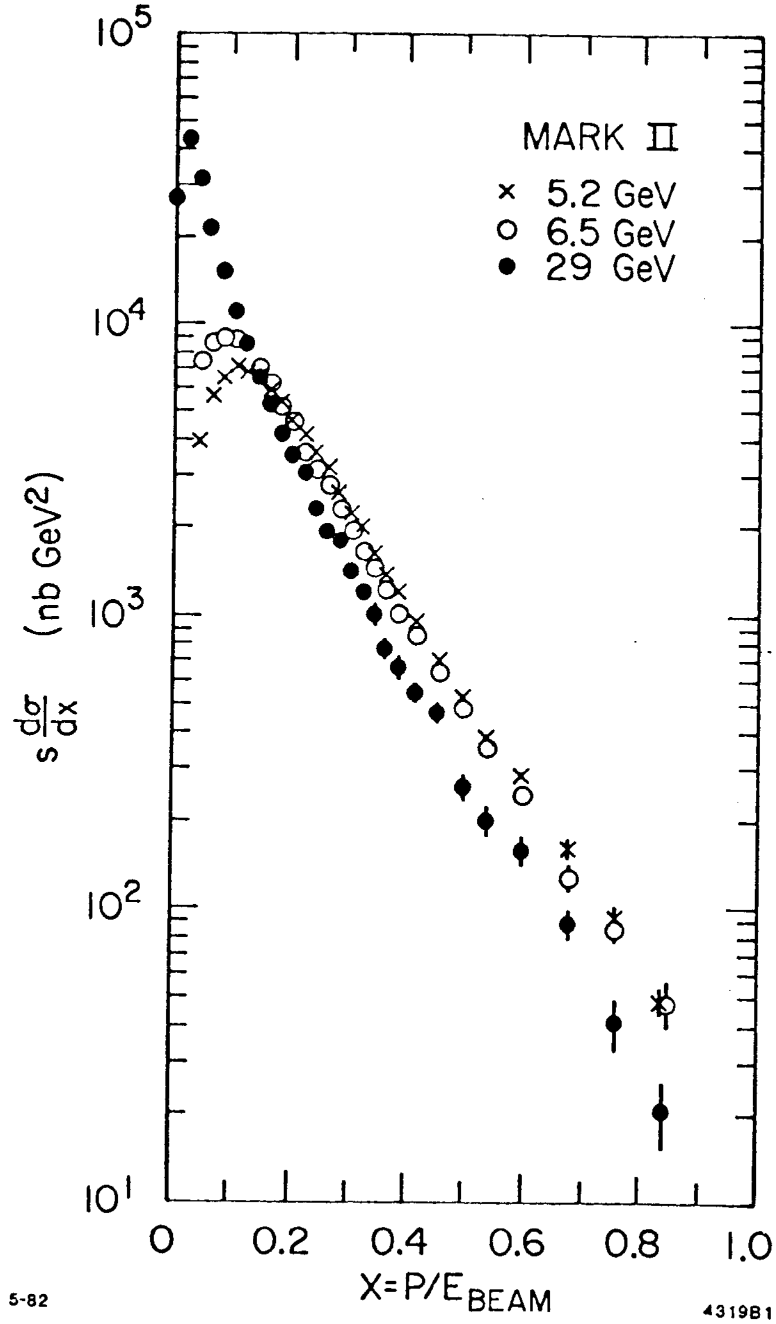

MARK II
× 5.2 GeV
○ 6.5 GeV
● 29 GeV
10^5
10^4
10^3
10^2
10^1
$s\frac{d\sigma}{dx}$ (nb GeV^2)
0
0.2
0.4
0.6
0.8
1.0
$X=P/E_{BEAM}$
5-82
4319B1

Fig. 1

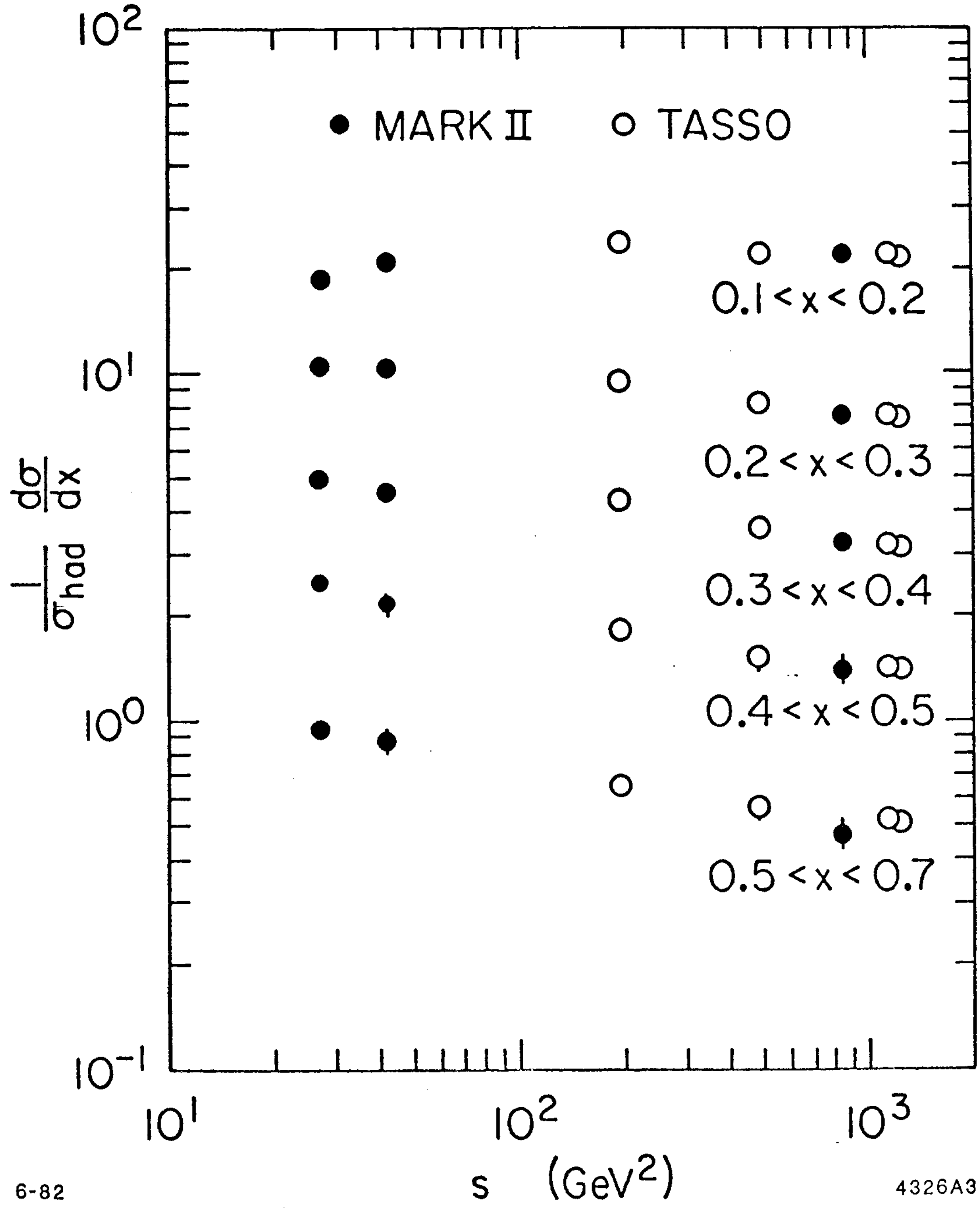

● MARK II
○ TASSO
0.1 < x < 0.2
0.2 < x < 0.3
0.3 < x < 0.4
0.4 < x < 0.5
0.5 < x < 0.7
$\frac{1}{\sigma_{had}} \frac{d\sigma}{dx}$
10^{2}
10^{1}
10^{0}
10^{-1}
10^{1}
10^{2}
10^{3}
s (GeV^2)
6-82
4326A3

Fig. 2

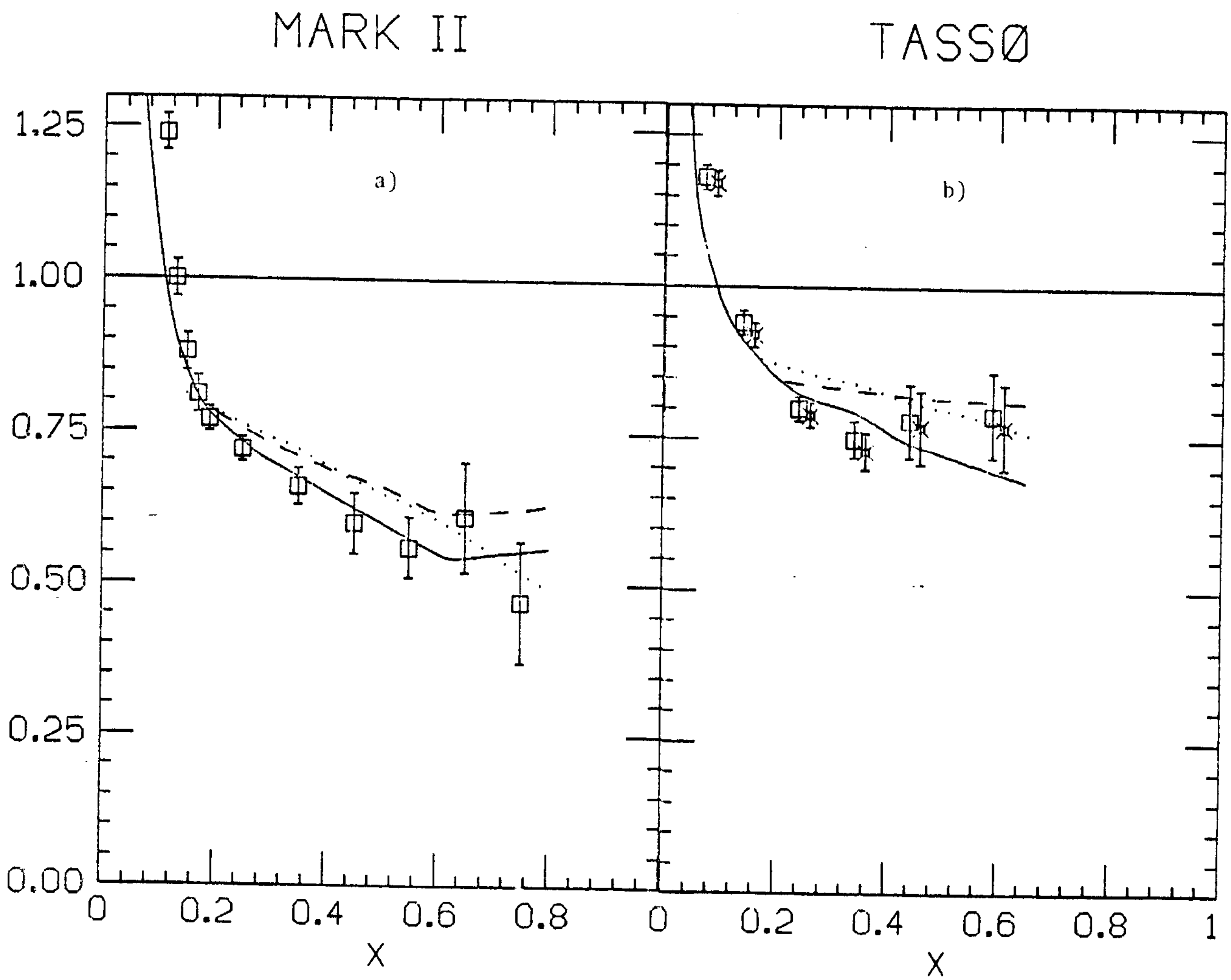

Fig. 3

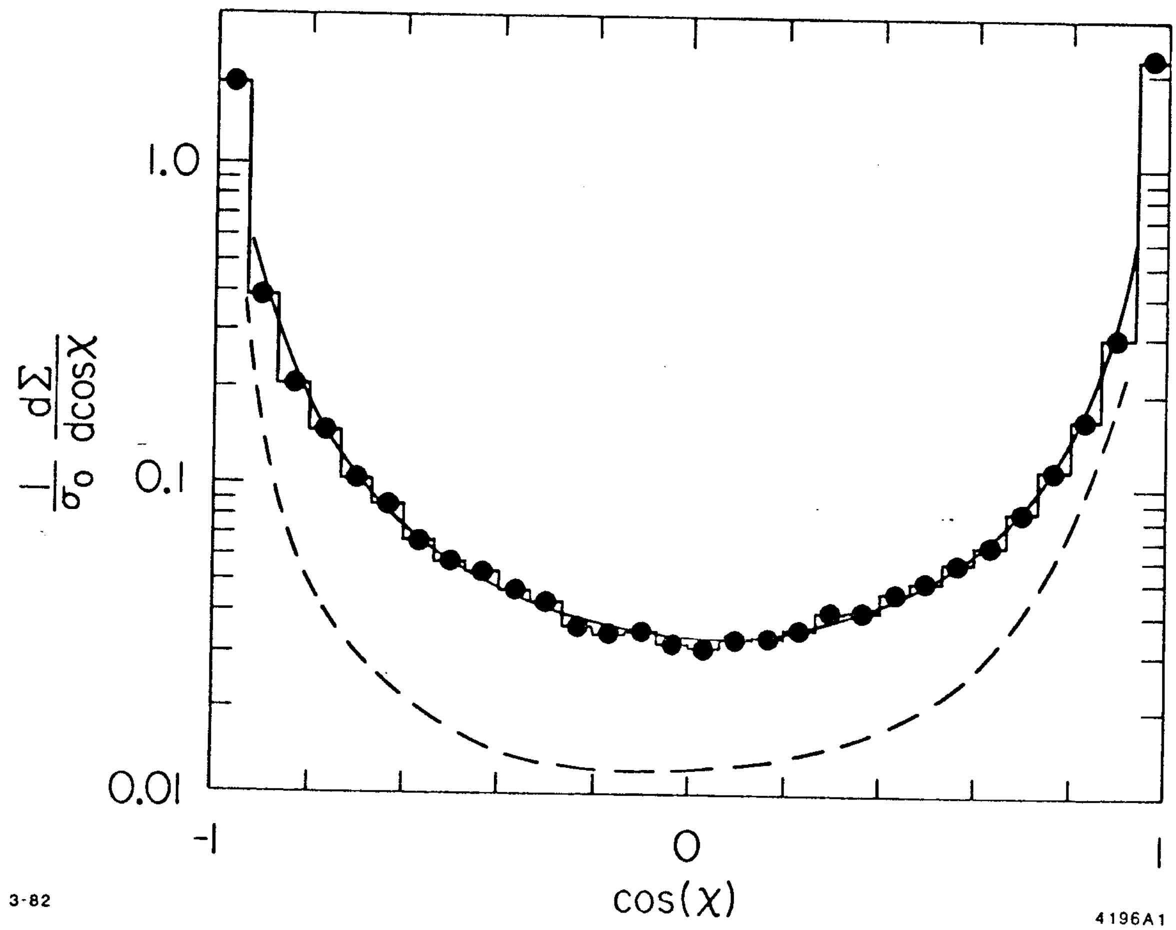

1.0
0.1
0.01
$\frac{1}{\sigma_0} \frac{d\Sigma}{d\cos\chi}$
-1
0
1
cos(χ)
3-82
4196A1

Fig. 4

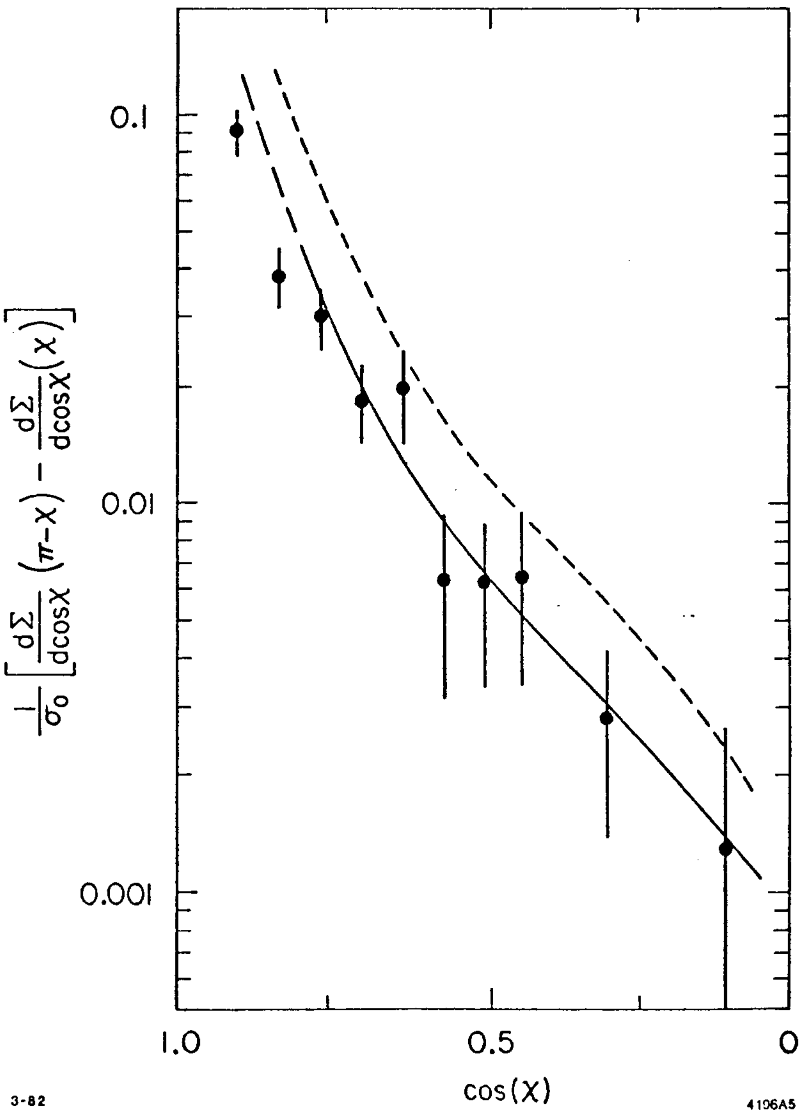

0.1
0.01
0.001
$\frac{1}{\sigma_0}\left[\frac{d\Sigma}{d\cos\chi}(\pi-\chi)-\frac{d\Sigma}{d\cos\chi}(\chi)\right]$
1.0
0.5
0
cos(χ)
3-82
4196A5

Fig. 5

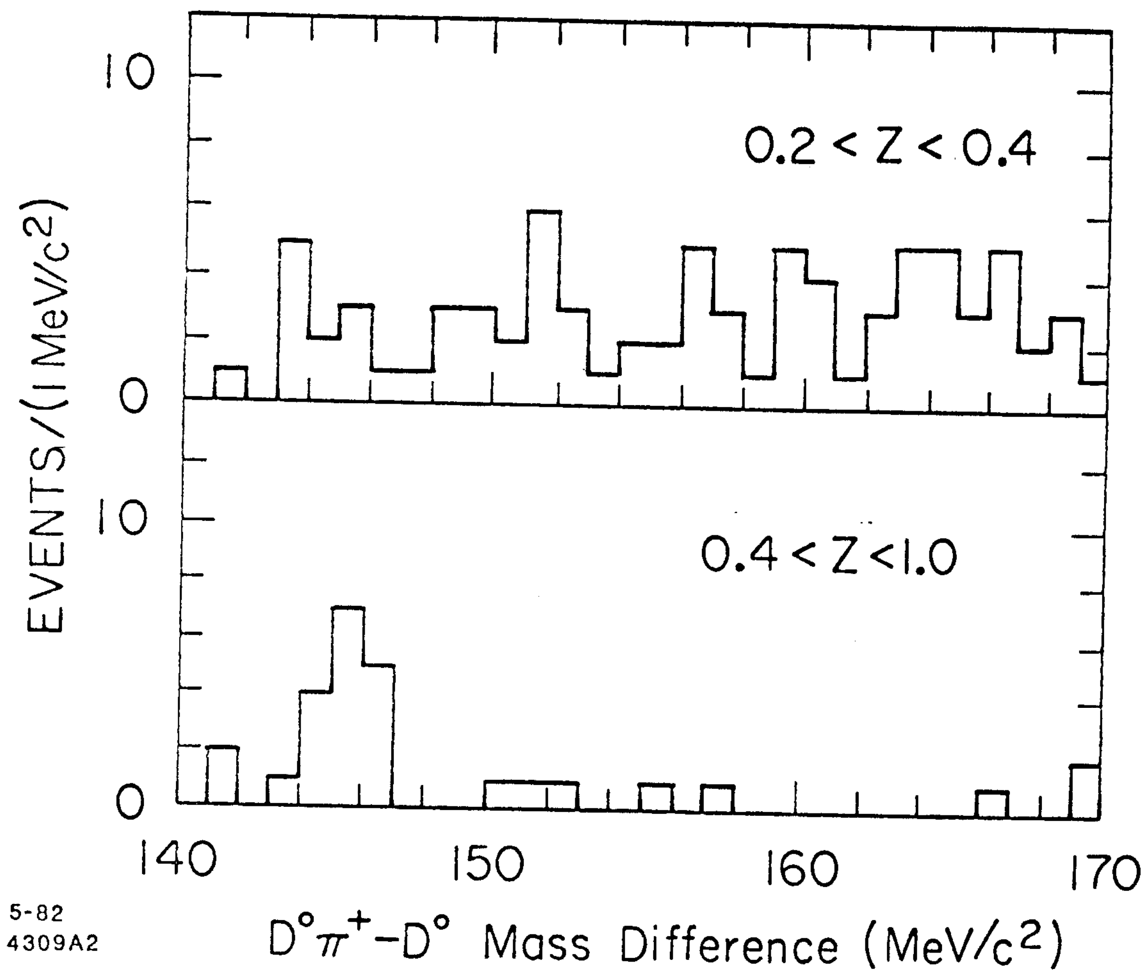

10
0.2 < Z < 0.4
EVENTS/(1 MeV/c2)
0
10
0.4 < Z < 1.0
0
140
150
160
170
5-82
4309A2
D°π+−D° Mass Difference (MeV/c2)

Fig. 6

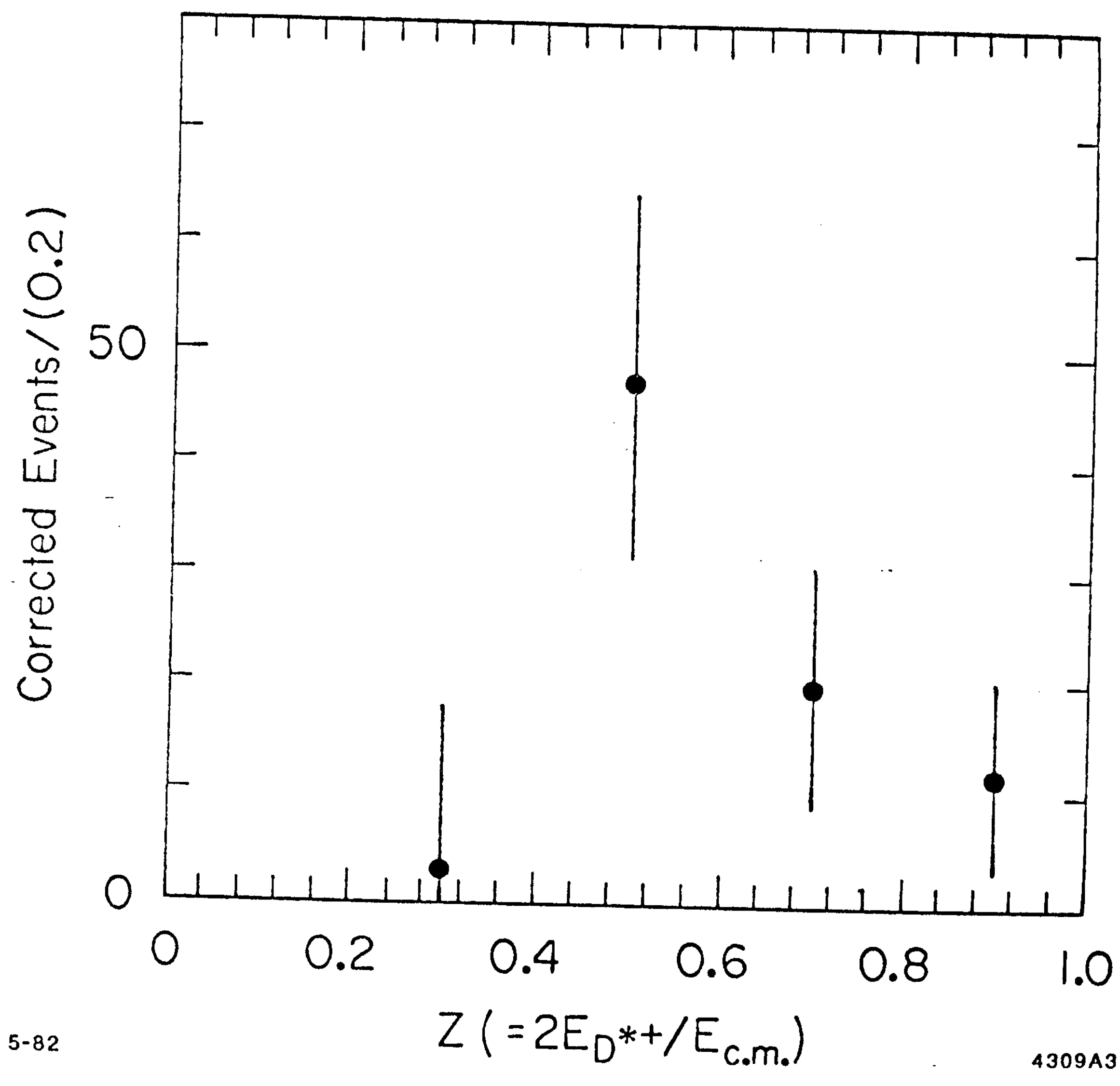

Fig. 7

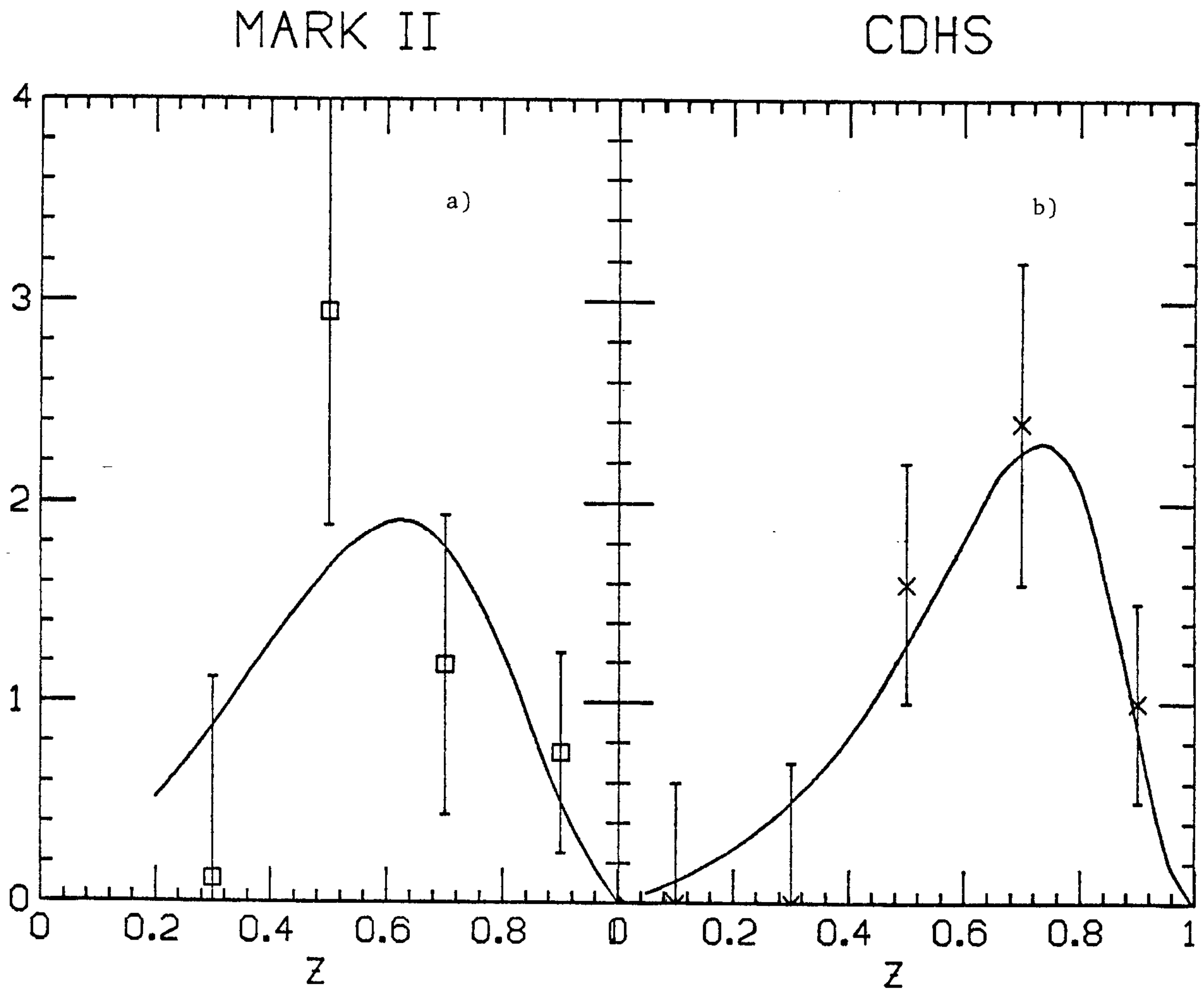

Fig. 8